

Cellular Uptake of a Polypyridyl Ruthenium Complex Revealed Using a Fluorescent Rhodamine-modified Ruthenium Complex

Yu-Ru Jhou,^a Chien-Hui Chiou,^a Lin-Kia Ni,^a Li-Chou Chen,^a Yau-Hung Chen^b and Chien-Chung Cheng^{a,*}^aDepartment of Applied Chemistry, National Chia-Yi University, Chia-Yi City, Taiwan 60004, R.O.C.^bDepartment of Chemistry, Tamkang University, Tamsui, Taipei, Taiwan, R.O.C.

(Received: Mar. 28, 2012; Accepted: May 28, 2012; Published Online: ??; DOI: 10.1002/jccs.201200172)

A fluorescent polypyridyl ruthenium complex was successfully prepared using an amide bond linkage to link two rhodamine moieties through bipyridine groups. Although photo-induced electron transfer (PET) quenched the fluorescent intensity, the quantum yield of the rhodamine-modified Ru(II) complex was 0.17 in water, sufficient for observing the fluorophore behaviour in biological systems. The rhodamine-modified Ru(II) complex was found to inhibit the bacterial growth of *E. coli*. In vitro fluorescence images of human hepatoma cells (SK-Hep1) showed that a fluorescent polypyridyl ruthenium complex not only supported the above observation but also preferably accumulated in the cytoplasmic region inside the cell. These observations suggest that in addition to strong Ru–DNA interactions, Ru–protein interactions in the cytoplasmic regions are strong and are therefore important to the development of metallopharmaceuticals.

Keywords: Ruthenium; Rhodamine; Polypyridine; Uptake; Fluorescence.

The development of imaging sensors for metal ions can facilitate investigations into the biological behavior of metal ions.^{1,2} Fluorophores associated with metal ions, such as Zn(II),^{3,4} Ca(II),^{5,6} or Cu(I)/(II),⁷⁻⁹ have been used to study the role of these metals in brain function and muscle action. Many synthetic metal complexes containing metal ions, such as platinum, bismuths, and gold, are not required for daily life but are important in the treatment and/or diagnosis of diseases.¹⁰ A better understanding of their interaction modes and pathways may guide the development of improved therapeutics. Recently, ruthenium complexes have been considered as alternatives to platinum drugs in antitumor therapy.¹⁰⁻¹² The synthetic polypyridyl chlororuthenium complexes constitute one class of potential antitumor reagents. Unlike Ru(III) ionic species generated from [Ru(Im)(DMSO)Cl₄][−] (Im: imidazole),¹³⁻¹⁵ polypyridyl chlororuthenium complexes are believed to exert antitumor activity as an integral metal complex.¹¹ In addition to Ru(II)–DNA interactions,^{13,16} the cytotoxicity of polypyridyl ruthenium complexes has been studied in murine and human tumour cells in vitro, and the bio-reactivity of the complexes has been evaluated in zebrafish embryos, revealing that the complex targets proliferating fin mesenchymal cells.¹⁷ The transport of polypyridyl ruthenium complexes through *E. coli* cell membranes was found to be related to stress-regulating proteins (the outer mem-

brane proteins, *OmpF*), in a study that employed proteomics techniques in conjunction with ICP-OES mass spectrometry.¹⁸ A systematic study of the inductive properties of polypyridyl ruthenium complexes showed that these complexes significantly influence the total cellular protein distribution, which can affect several metabolic pathways in *E. coli*. The main biological processes associated with the down-regulated proteins were related to carbohydrates, including transport, the tricarboxylic acid (TCA) cycle, glycolysis, and gluconeogenesis.¹⁹ This work suggests that Ru–protein interactions in the cytoplasm contribute significantly to the modulation of cell growth, in addition to the effects of Ru–DNA interactions in the cell nuclei. Visualization of ruthenium complex localization inside cells would assist in differentiating the effects of interactions with genomic DNA or cytoplasmic protein.

One approach to visualizing the in vitro localization of ruthenium complexes involves introducing a fluorescent group to a ruthenium complex. [Ru(terpy)(dppz)Cl]⁺ (terpy: terpyridine, dppz: dipyrido[3,2-*a*:2',3'-*c*]phenazine) and its analogues have been developed as potential candidate fluorescent ruthenium complexes.²⁰ The electronic state absorption properties and DNA affinity of [Ru(terpy)-(dppz)Cl]⁺ have been well characterized; however, the binding affinity of this complex may be heavily influenced by the high affinity of dppz toward DNA via π – π interac-

* Corresponding author. Tel: +886-5-2766084; Fax: +886-5-2717901; E-mail: cccheng@mail.ncyu.edu.tw

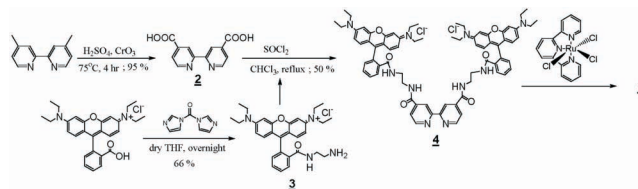
tions of the aromatic rings.²¹

An alternative visualization approach involves the linking of fluorophores containing a modified bipyridine at the 4,4'-position to generate a fluorescent ruthenium complex,²² as shown in Figure 1. This paper describes the preparation of a fluorescent ruthenium complex into which a rhodamine-modified bipyridine moiety has been introduced to link two rhodamine moieties through an amide bond. The rhodamine moiety was selected for introduction into the framework of the ruthenium complexes due to its reasonable solubility in water, relative chemical inertness in biological systems, and acceptable quantum yield for fluorescence visualization. The ruthenium complex was characterized by NMR and mass spectroscopy. Visualization of the fluorescent ruthenium complex localization was accomplished by fluorescence imaging of human hepatoma cells (SK-Hep1). The large rhodamine-modified Ru(II) complex appeared to be transportable into SK-Hep1 cells, and it accumulated mainly in the cytoplasm.

Compound **1** was prepared by synthesizing the rhodamine-modified bipyridine, **4**, followed by a reaction with Ru(terpy)Cl₃ in EtOH for 18 hr, as shown in Scheme I. The preparation of a rhodamine-modified bipyridine was achieved by the following procedure. The rhodamine derivative, **3**, was prepared with an N-terminus by coupling a carboxylic group to an ethylenediamine moiety in the presence of 1,1-carbonyldiimidazole (CDI) under anhydrous conditions with a yield of 66%.²³ 4,4'-Dicarboxylate bipyridine, **2**, was reacted with thionyl chloride under reflux conditions for 4 hr to form the diacyl chloride derivative for use in the next step. Compound **4** was produced by the slow addition of the diacyl chloride derivative in a CHCl₃ solution to a CHCl₃ solution of the rhodamine derivative, **3**, at room temperature. The reaction was then refluxed for an additional 5 hr to obtain a deep purple-red solid in a yield of 50%. The fluorescent ruthenium complex, **1**, was prepared according to the previously reported procedure²⁴ by re-

fluxing compound **4** with Ru(terpy)Cl₃ in an ethanolic solution in the presence of LiCl and triethylamine to give a deep brown-red precipitate in a yield of 24%.

Scheme I Synthesis of a rhodamine-modified ruthenium complex via amide bond linkage



The rhodamine-modified ruthenium complex was characterized by solution NMR and MALDI mass spectroscopy. Because the ruthenium center was divalent and diamagnetic, compound **1** displayed distinct peaks in the NMR spectrum. The chemical shifts of compound **1** were affected by the ring current effects of the terpyridine ligand, so the chemical shifts of the pyridine moieties in the bipyridine derivative differed from one another. Compound **1** displayed asymmetric proton shifts in the bipyridine ligand, which complicated the assignment of the proton NMR spectrum. To deconvolute the chemical structures, compounds **1** and **4** were analysed by ¹H-COSY NMR techniques. The assignment of compound **1** is illustrated in Figure 2. One of the 7-positions of the bipyridine ligand showed a downfield shift from 8.76 ppm in the rhodamine-modified bipyridine to 10.12 ppm in the ruthenium complex. The peak at 1.36 ppm suggested the presence of ring current effects due to the terpyridine in compound **1**. The formation of a ruthenium complex was confirmed by analysis of the MALDI mass spectra, which revealed a molecular ion peak, [M]⁺, with a mass-charge ratio (*m/z*) of 1546.4.

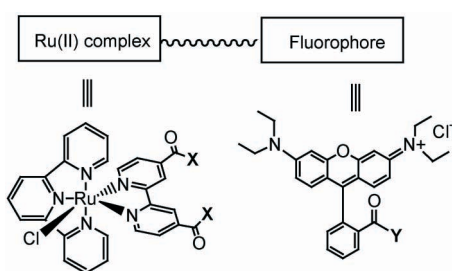


Fig. 1. Design of a rhodamine derivative of a fluorescent Ru complex.

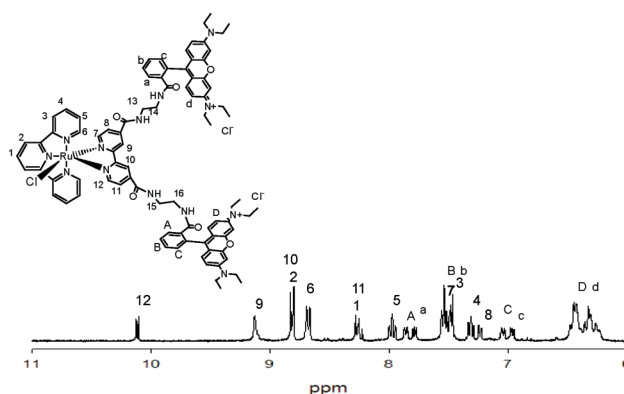
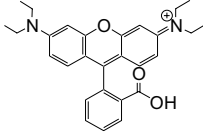
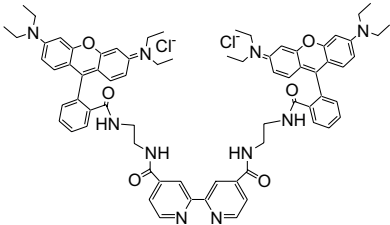
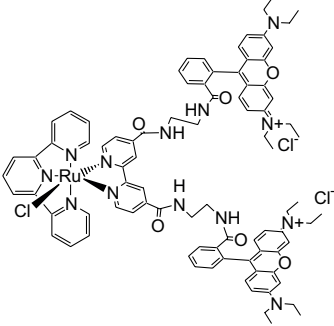


Fig. 2. ¹H-NMR spectrum of compound **1**.

Table 1. UV-vis spectroscopic comparison of the ligands and the corresponding ruthenium complex, showing the absorption wavelength, absorption coefficients, emission wavelength, and quantum yield

Structure			
Compound	Rhodamine B	4	1
λ_{\max} (nm)(ϵ M ⁻¹ cm ⁻¹)	553 (107000)	557 (145551) ^[a] 548 (317085)/(MeOH)	557 (15380) 547 (1509919)/(MeOH)
λ_{em} (λ_{ex}) (nm)	572 (500)	575 (536)	574 (536)
Φ	0.48 (water); 0.80 (MeOH)	0.35 (water)	0.17 (water)

^[a] H₂O, pH 2

The electronic spectra of the fluorescent ruthenium complex were measured in support of the physical characterization studies of compound **1**. The electronic absorption spectrum of compound **1** showed an absorption band at a wavelength of 547 nm in methanol, which was comparable to the absorption at 548 nm for compound **4**, and 553 nm for rhodamine B. These results suggested that the electronic structure of the dye was not significantly affected by the bipyridine linkage, as shown in Table 1. The emission spectrum of compound **1** revealed an emission band at 574 nm in water upon excitation at 536 nm. The emission spectra of the ligand, compound **4**, and rhodamine 6B were similar. However, the emission intensity of compound **1** in water was dramatically reduced by a factor of 2 relative to the emission intensity of rhodamine-modified bipyridine. Fluorescence can be easily quenched in aqueous solutions or transition metal ions containing d-orbital electrons; e.g., Ni(II), Cu(II), and Ru(II) ions.²⁵ Therefore, the fluorescence intensity of compound **1** was inevitably quenched to a certain degree by the presence of ruthenium ions. The quantum yield of compound **1** was reduced to 0.17 in water; however, this quantum yield was sufficient for visualization studies in biological systems.

The large volume of compound **1**, which included a ruthenium complex and two rhodamine moieties, could potentially prevent transport into cells. The diameter of the ruthenium complex was estimated to increase from 13 Å

for [Ru(terpy)(dmbpy)Cl]⁺ (dmbpy: 4,4'-dimethylbipyridine) to 23–36 Å for compound **1**. The transport properties of compound **1** were evaluated in the context of BL21 cell growth inhibition, as reported previously. Compound **1** was found to have an inhibition concentration (IC₅₀) of 60 μM, comparable to that measured for the [Ru(terpy)(dmbpy)Cl]⁺ complex under similar conditions. The outer membrane protein (*ompF*) involved in [Ru(terpy)(dmbpy)Cl]⁺ transport in *E. coli* is also involved in stress-regulation processes.¹⁸ The X-ray structure of *ompF* revealed a trimeric protein structure in which each monomer was approximately cylindrical with a radius of 30 Å.²⁶ This suggests that it was reasonable for compound **1**, with a large volume of rhodamine moieties, to penetrate *E. coli* cells through the stress-regulation pathway. The concentration of compound **1** in the cell media could not be increased without producing a red precipitate. Compound **1** apparently has limited solubility in water, possibly due to the hydrophobicity of the aromatic rings.

SK-Hep1 cells were used in fluorescence imaging experiments to visualize the localization of compound **1** inside cells. SK-Hep1 cells were cultured in LDF medium containing 10 ppm compound **1** for 24 hr at 37 °C. Red fluorescence due to compound **1** was observed primarily in the cytoplasm, as shown in Figure 3. A control reaction involving staining with rhodamine 6B yielded with nonspecific location in SK-Hep 1 cells. Under similar conditions,

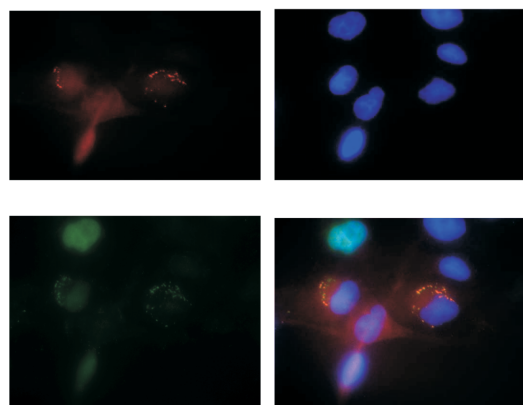


Fig. 3. Fluorescent imaging of SK-Hep1 cells. (A) Staining with compound **1** (red fluorescence); (B) staining with DAPI (blue fluorescence) to visualize the nuclei; (C) expression levels of P21 detected with mouse anti-human P21 (1:1000; Santa Cruz) as a primary antibody, and with Alexa Fluor 488 rabbit anti-mouse-IgG (1:200; Molecular Probes) as the secondary antibody (green fluorescence); and (D) merged signal (orange fluorescence), indicating overlap between the signals corresponding to compound **1** (red) and P21 (green).

SK-Hep1 cells were counter-stained with 4',6-diamidino-2-phenylindole (DAPI, excitation wavelength at 358 nm/emission wavelength at 461 nm), which yields a blue fluorescence and binds strongly to A-T rich regions in DNA, to visualize the nuclei of the SK-Hep1 cells, as shown in Figure 3B. A comparison of the fluorescence images suggested that the red fluorescence of compound **1** was not significantly accumulated in the nuclei.^{27,28} Compound **1**-treated SK-Hep1 cells were stained with a green fluorescent protein-labelled mouse anti-human P21 antibody, as shown in Figure 3C, to visualize the expression of P21. The yellow fluorescence of the antibody overlaid with the fluorescence of compound **1**, suggesting that compound **1**-treated SK-Hep1 cells induced P21 expression and resulted in apoptosis.²⁹ As a result, compound **1** not only was internalized by the cells, but it predominantly accumulated in the cytoplasm region.

In summary, a fluorescent ruthenium complex was successfully prepared by linking two rhodamine moieties to the complex via an amide bond. Despite its large volume, compound **1** was transported into cells, where it was found to inhibit *E. coli* growth. Fluorescence images of SK-Hep1 cells incubated with compound **1** revealed that the polypyridyl ruthenium complex preferably accumulated in the

cytoplasm. The possibility that compound **1** was too large in size to transport into the nucleus could not be excluded. Fluorescence imaging suggested that the Ru-protein interactions in the cytoplasm were important for bacterial growth inhibition; Ru-DNA interactions in the nuclei may also play a role in this regard. This work provides a new fluorescence visualization tool to assist in the development of ruthenium-based metallopharmaceuticals.

ACKNOWLEDGEMENT

The authors thank the Academia Sinica in Taiwan for kindly providing the mass spectroscopy facilities. We gratefully acknowledge the financial support of the National Science Council of the Republic of China.

REFERENCES

- Domaille, D. W.; Que, E. L.; Chang, C. J. *Nat. Chem. Biol.* **2008**, *4*, 168.
- Terai, T.; Nagano, T. *Curr. Opin. Chem. Biol.* **2008**, *12*, 515-21.
- Kimura, E.; Aoki, S. *BioMetals* **2001**, *14*, 191.
- Tomat, E.; Lippard, S. J. *Curr. Opin. Chem. Biol.* **2010**, *14*, 225.
- Tsien, R. Y. *Biochemistry* **1980**, *19*, 2396.
- Mac, M.; Uchacz, T.; Danel, A.; Danel, K.; Kolek, P.; Kulig, E. *J. Fluorescence* **2011**, *21*, 375.
- Neupane, L. N.; Thirupathi, P.; Jang, S.; Jang, M. J.; Kim, J. H.; Lee, K.-H. *Talanta* **2011**, *85*, 1566.
- Liu, Z.-C.; Yang, Z.-Y.; Li, T.-R.; Wang, B.-D.; Li, Y.; Qin, D.-D.; Wang, M.-F.; Yan, M.-H. *Dalton Trans.* **2011**, *40*, 9370.
- Vinkenborg, J. L.; Koay, M. S.; Merckx, M. *Curr. Opin. Chem. Biol.* **2010**, *14*, 231.
- van Rijt, S. H.; Sadler, P. J. *Drug Discovery Today* **2009**, *14*, 1089.
- Antonarakis, E. S.; Emadi, A. *Cancer Chemother. Pharmacol.* **2010**, *66*, 1.
- Clarke, M. J. *Coordination Chem. Rev.* **2003**, *236*, 209.
- Brabec, V.; Nováková, O. *Drug Resistance Updates* **2006**, *9*, 111.
- Pluim, D.; van Waardenburg, R. C. M.; Beijnen, J. H.; Schellens, J. H. M. *Cancer Chemother. Pharmacol.* **2004**, *54*, 71.
- Casini, A.; Mastrobuoni, G.; Terenghi, M.; Gabbiani, C.; Monzani, E.; Moneti, G.; Casella, L.; Messori, L. *J. Biol. Inorg. Chem.* **2007**, *12*, 1107.
- Cheng, C. C.; Lee, W. L.; Su, J. G.; Liu, C. L. *J. Chin. Chem. Soc.* **2000**, *47*, 213.
- Wang, Y. H.; Cheng, C. C.; Lee, W. J.; Chiou, M. L.; Pai, C. W.; Wen, C. C.; Chen, W. L.; Chen, Y. H. *Chem-Biol. Inter-*

- act.* **2009**, *182*, 84.
18. Ho, M.-Y.; Chiou, M.-L.; Chang, R.-C.; Chen, Y.-H.; Cheng, C.-C. *J. Inorg. Biochem.* **2010**, *104*, 614.
19. Ho, M.-Y.; Chiou, M.-L.; Du, W.-S.; Chang, F. Y.; Chen, Y.-H.; Weng, Y.-J.; Cheng, C.-C. *J. Inorg. Biochem.* **2011**, *105*, 902.
20. Kalsbeck, W.; Thorp, H. H. *J. Am. Chem. Soc.* **1993**, *115*, 7146.
21. Zeglis, B. M.; Pierre, V. C.; Barton, J. K. *Chem. Commun.* **2007**, 4565.
22. Garelli, N.; Vierling, P. *J. Org. Chem.* **1992**, *57*, 3046.
23. Chen, Y.-H.; Chiou, C.-H.; Chen, W.-L.; Jhou, Y.-R.; Lee, Y.-T.; Cheng, C.-C. *J. Chin. Chem. Soc.* **2010**, *57*, 1257.
24. Konno, H.; Ishii, Y.; Sakamoto, K.; Ishitani, O. *Polyhedron* **2002**, *21*, 61.
25. Posokhov, Y. O.; Kyrychenko, A.; Ladokhin, A. S. *Anal. Biochem.* **2010**, *407*, 284.
26. Cowan, S.; Garavito, R.; Jansonius, J.; Jenkins, J.; Karlsson, R.; König, N.; Pai, E.; Pauptit, R.; Rizkallah, P.; Rosenbusch, J.; Rummel, G.; Schirmer, T. *Structure* **1995**, *3*, 1041.
27. Tian, X.; Gill, M. R.; Cantón, I.; Thomas, J. A.; Battaglia, G. *Chembiochem.* **2011**, *12*, 548.
28. Fernández-Moreira, V.; Thorp-Greenwood, F. L.; Coogan, M. P. *Chem. Commun.* **2010**, *46*, 186.
29. Peng, H. C.; Wang, Y. H.; Wen, C. C.; Wang, W. H.; Cheng, C. C.; Chen, Y. H. *Comp. Biochem. Physiol. C: Toxicol. Pharmacol.* **2010**, *151*, 480.